

RSC Advances



This is an *Accepted Manuscript*, which has been through the Royal Society of Chemistry peer review process and has been accepted for publication.

Accepted Manuscripts are published online shortly after acceptance, before technical editing, formatting and proof reading. Using this free service, authors can make their results available to the community, in citable form, before we publish the edited article. This *Accepted Manuscript* will be replaced by the edited, formatted and paginated article as soon as this is available.

You can find more information about *Accepted Manuscripts* in the [Information for Authors](#).

Please note that technical editing may introduce minor changes to the text and/or graphics, which may alter content. The journal's standard [Terms & Conditions](#) and the [Ethical guidelines](#) still apply. In no event shall the Royal Society of Chemistry be held responsible for any errors or omissions in this *Accepted Manuscript* or any consequences arising from the use of any information it contains.

Fast Co-Pyrolysis of Cellulose and Polypropylene Using Py-GC/MS and Py-FT-IR

Deepak Kumar Ojha ^a and R. Vinu ^{a,b,*}

^a Department of Chemical Engineering, Indian Institute of Technology Madras, Chennai-600036, India

^b National Center for Combustion Research and Development, Indian Institute of Technology Madras, Chennai- 600036, India

* Corresponding Author, Phone: +91-44-2257 4178, E-mail: vinu@iitm.ac.in (R. Vinu)

Abstract

In this study, the production of high quality biofuel intermediates via fast co-pyrolysis of cellulose and polypropylene (PP) is investigated. Fast co-pyrolysis experiments were performed in Pyroprobe[®] reactor and the generated vapors were analyzed using gas chromatograph-mass spectrometer for composition of pyrolysates, and Fourier transform infrared spectrometer for time evolution of key functional groups. The effects of cellulose to PP mass ratio (100:0, 75:25, 50:50, 25:75, 0:100) and temperature (500-800°C) on bio-oil composition, carbon number distribution of the products, higher heating value of the products, and temporal evolution of –OH, C-O, -CH₂-, CO₂ and C=O groups are evaluated. Formation of long chain alcohols in the carbon number range of C8-C20 is observed as a result of interaction of cellulose and PP. Feed composition plays a decisive role on the production of alcohols and hydrocarbons. A maximum of c.a. 36% alcohols and 45% hydrocarbons were obtained from PP-rich mixture at 600 °C. The yield of char decreased and that of aromatic hydrocarbons increased with pyrolysis temperature. Significant improvement in the heating value of the products is observed when PP is blended with cellulose. Importantly, the calculated heating values correlated well with the cumulative content of alcohols, aliphatic and aromatic hydrocarbons. The addition of PP to cellulose was also found to significantly decrease the time taken for completion of pyrolysis. Based on the product distribution, hydroxyl, hydrogen and methyl abstraction were found to be the dominant reactions involved in the transformations.

Keywords: Fast co-pyrolysis; cellulose; polypropylene; Py-GC/MS; Py-FTIR; long chain alcohols

1. Introduction

Fast pyrolysis is a promising technology for producing carbon neutral fuel and intermediates from lignocellulosic biomass. The technique involves pyrolyzing the sample at moderate temperature (400-600 °C) at very high heating rates ($>1000 \text{ }^\circ\text{C s}^{-1}$), which leads to the production of condensable vapors or bio-oil in high yields (60-70 wt.%).¹ The estimated energy density of the pyrolysis oil can be four to seven times the overall energy density of the biomass alone.² Apart from the pyrolysis conditions, the composition of crude bio-oil depends on the relative amount of cellulose, hemicelluloses, lignin and ash in the biomass. The cellulose and hemicellulose are converted to 5-hydroxymethyl furfural, furfural and furan derivatives, carboxylic acids, aldehydes and anhydrosugars, lignin is converted to phenolics and aromatic hydrocarbons, and ash plays a catalytic role in the entire process.³ Owing to the presence of oxygenated organics, pyrolysis oil is inherently unstable and its overall composition varies with time.⁴ The high concentration of oxygen (28-50 wt.%) in the form of water (15-30 wt.%) and various oxygenates makes the bio-oil acidic (pH 2-4), lowers its heating value and flame temperature, and enhances its fluidity.^{1,5}

Bio-oil upgradation to drop-in fuels and intermediates is achieved by two common techniques, namely, catalytic upgrading and hydrodeoxygenation. Catalytic upgrading involves fast pyrolyzing the feedstock in presence of catalysts such as zeolites, transition metal oxides or mesoporous materials.^{1,6} Hydrodeoxygenation (HDO) involves removal of oxygen from the feedstock by passing hydrogen gas at high pressures in presence of hydrotreating catalysts such as bifunctional Co-Mo/Al₂O₃.^{7,8} This upgrading technique is capable of removing more than 90% of oxygen in the feedstock to produce gasoline and diesel range fuels. However, the process is highly hydrogen intensive and has shortcomings of catalyst deactivation. Furthermore, if the

operating conditions are not optimized properly, the competing polymerization reaction of dehydrated intermediates leads to the formation of high molecular weight compounds and char/coke.⁹

Co-feeding hydrogen-rich thermoplastic polymers along with oxygen-rich biomass is a potential strategy to improve the quality of bio-oil, especially the H/O ratio. This also paves way for a better utilization of waste plastics that constitute a major fraction of municipal solid wastes.¹⁰ Even partial removal of oxygen in the bio-oil can significantly reduce the consumption of hydrogen in the HDO step. Besides, this also improves the stability of bio-oil. The presence of olefinic polymers is thought to induce hydrogen abstraction reactions between the long chain polymer species and free radicals produced from biomass intermediates.¹¹ The elementary reactions occurring in the melt phase during fast pyrolysis include a number of competing free radical, ionic and concerted reactions of cellulose, hemicelluloses, lignin, ash and polymeric species. While olefinic polymers are well known to decompose via a cascade of free radical reactions,¹² the specific reactions involved in the transformation of biomass components are largely unclear.¹³ Therefore, it is very important to characterize the co-pyrolysis behavior of pure components of biomass and polymers using various analytical techniques.

Co-pyrolysis of biomasses, such as cellulose, xylan, lignin, switch grass, pine, beech and spruce woods, with polymers, such as polystyrene, polyethylenes, polypropylene (PP), poly(ethylene terephthalate), poly(vinyl chloride) (PVC) and tyres is reported in the literature.^{10,11,14-24} In a series of studies, Sharypov and co-workers^{11,14-16} evaluated the effects of feed composition and additives on the product yield and quality during co-pyrolysis of biomass and polymers in a rotating autoclave. It was found that the product evolution was additive when biomass composition in the feed was 50-100%, while higher plastic content made the product

evolution non-additive. The higher liquid and lower char yield were attributed to the hydrogen transfer reaction from polyolefins to biomass radicals that tend to stabilize the primary products from cellulose degradation. Mullen and co-workers^{21,22} studied catalytic fast co-pyrolysis of biomass with polymers using HZSM-5, and observed a synergism in the formation of aromatic compounds like toluene, ethylbenzene, xylenes and naphthalenes via Diels Alder reactions. In another recent study of fast co-pyrolysis of biomass components with PVC, the interactions were found to decrease the HCl yield and improve tar yield.²⁴ Recently, we evaluated the kinetics of slow co-pyrolysis of cellulose and PP using thermogravimetric analyzer, and showed that the interactions between the primary volatiles from cellulose with activated PP decrease the apparent activation energy of the process.¹⁰ While the existing studies demonstrate the positive effects of co-pyrolysis on overall product spectrum, the exact mechanism and interactions between biomass and polymers are largely unclear owing to the presence of a large number of competing reactions. Moreover, the effect of co-pyrolysis on pyrolysis time scales is also not known.

The present work aims to unravel the key interactions between cellulose and PP during non-catalytic fast co-pyrolysis using analytical pyrolyser (Py) coupled with high resolution gas chromatograph-mass spectrometer (GC/MS) and Fourier transform infrared spectroscopy (FT-IR). The effects of feed composition and temperature on the evolution of pyrolysates are evaluated. The quality of the pyrolysates obtained under different conditions is assessed by evaluating the carbon number distribution and heating value. The evolution of the key functional groups at short time scales during fast co-pyrolysis is studied using Py-FT-IR, and plausible reaction mechanism is proposed.

2. Experimental

2.1 Materials

Microcrystalline cellulose powder (particle size $\sim 50 \mu\text{m}$, $M_n = 135,554 \text{ g mol}^{-1}$,¹² polydispersity index = 2.25) and atactic PP ($M_w \sim 14000 \text{ g mol}^{-1}$, $M_n \sim 3700 \text{ g mol}^{-1}$) were procured from Sigma Aldrich. The as-received PP was in the form of beads of size 4-10 mm. The PP beads were pressed and then cut into small pieces of size $< 500 \mu\text{m}$. The materials were preheated at $100 \text{ }^\circ\text{C}$ for an hour to remove physically bound moisture. The treated cellulose and PP were taken in different mass ratios, viz. 100:0 (pure cellulose), 75:25, 50:50, 25:75, 0:100 (pure PP), and thoroughly mixed in a mortar before subjecting to fast pyrolysis.

2.2 Py-GC/MS Experiments

Fast pyrolysis experiments were performed in a Pyroprobe[®] 5200 pyrolyzer (CDS Analytical, U.S.A.). Approximately $500 \pm 30 \mu\text{g}$ of the sample was taken in the quartz tube and subjected to fast pyrolysis at a heating rate of $20 \text{ }^\circ\text{C ms}^{-1}$. The sample was then held at the desired temperature (500, 600, 700 or $800 \text{ }^\circ\text{C}$) for 50 s. The pyrolysates were thoroughly analyzed using two dimensional (2D)-GC/MS. The vapors were separated using two capillary connected in series using a pressure modulator with a modulation period of 20 s. Ultra high pure helium (99.99995%) was used as the carrier gas in splitless mode with 1 mL min^{-1} and 30.8 mL min^{-1} through the first and second columns, respectively. The injector, interface and ion source temperatures were set at 280, 300 and $230 \text{ }^\circ\text{C}$, respectively. GC column oven was held at $45 \text{ }^\circ\text{C}$ for 5 min, then heated at $5 \text{ }^\circ\text{C min}^{-1}$ to $240 \text{ }^\circ\text{C}$, and finally held at $240 \text{ }^\circ\text{C}$ for 2 min. The m/z range in the MS was 20-400 Da. The individual components were identified by comparing the mass spectra with NIST, Biofuel and Polymer libraries, and all the reported products had a high

match factor (700/1000). A similar match factor was also reported for 2D-GC/MS analysis of bio-oils.^{25,26} As more than 150 organic compounds were observed in each experiment, quantification of the individual organic compounds was performed by evaluating the area under the ion chromatogram peaks in terms of pixel counts. The area% was further normalized with respect to (100 – char wt.%). Char quantity was measured gravimetrically using a high accuracy microbalance (Sartorius Cubis). A majority of the experiments were repeated thrice, and the standard deviation in peak areas of the organic groups was in the range of 7-15%. Figure S1 (in supplementary data) depicts the typical 2D-GC/MS total ion chromatogram obtained from fast co-pyrolysis of equal composition mixture of cellulose and PP.

2.3 Py-FT-IR Experiments

In order to probe the progress of fast pyrolysis in terms of the evolution of functional groups and typical reaction times, the vapor phase products were scanned using FT-IR spectrometer equipped with a high sensitivity MCT detector. For these experiments, a Pyroprobe® 5150 pyrolyzer (CDS Analytical, U.S.A.) was interfaced with FT-IR spectrometer (Agilent Cary 660) via a Brill cell.²⁷ The Brill cell was placed in the path of IR beam in the sample compartment. The Brill cell was equipped with ZnSe windows, and the FT-IR spectra were collected in the range of 4000-600 cm^{-1} at the resolution of 2 cm^{-1} . The Brill cell interface was held at 200 °C and ultra high pure nitrogen was passed at a flow rate of 110 mL min^{-1} . The N_2 flow rate was optimized to ensure minimum deposition of pyrolysis vapors on the ZnSe windows.²⁸ A total sample quantity of 10 ± 0.2 mg was taken in the quartz tube. Owing to the high pyrolysis temperature (> 500 °C) inside the quartz tube and the high Brill cell temperature, condensation of the volatile products is not expected. Moreover, the volatilities of the products are not expected to be decreased. A snapshot of the Py-FT-IR set-up is depicted in Figure S2 (in

supplementary data). Ten FT-IR spectra of the vapor phase products were collected every second and analyzed. The non-condensable gases obtained at the exit of the FT-IR Brill cell were continuously monitored using a pre-calibrated gas analyzer (Bhoomi Analyzers, India).

3. Results and Discussion

3.1 Effect of Feed Composition on Product Spectrum

Fast pyrolysis of cellulose, PP and their mixtures in 75:25, 50:50 and 25:75 mass ratios were conducted in Py-GC/MS set-up at 500 °C. Fast pyrolysis of cellulose resulted in oxygenated compounds like anhydrosugars, furans, carbonyl compounds (aldehydes/ ketones), carboxylic acids and alcohols as the main products, while PP pyrolysis resulted in hydrocarbons as the only products. The identity and composition of various pyrolysates from cellulose and PP matched well with literature.^{20,29-31} The detailed list of products obtained from cellulose, PP and their mixtures, grouped into various categories are available in Tables S1-S6 (in supplementary data). Figure 1 depicts the composition of products grouped according to functional groups for various mixture compositions. Hydrocarbons are the major products from the mixtures, which is expected as they are formed from PP. Importantly, alcohols are formed as the major products of interaction between cellulose and PP. All other product groups such as anhydrosugars, aldehydes, ketones, furans and acids are produced in low quantities when the mixtures are pyrolyzed. Interestingly, an optimum amount of char is produced from the equal composition mixture. It was recently shown that the incorporation of PP in cellulose led to a decrease in char formation during slow pyrolysis, and highest production of char was evidenced with pure cellulose at heating rates in the range of 10-180 °C min⁻¹.¹⁰ The contrasting observations under fast pyrolysis conditions indicate that hydrocarbon vapors from PP might react with char

produced from cellulose to form condensed ring aromatic compounds that are retained in the solid residue after pyrolysis. More cellulose in the feed provides more fixed carbon, and hence, more surface for reaction of PP vapors, whereas more PP will generate more vapors. An alternate mechanism involving interaction of the primary volatiles from cellulose with activated polypropylene in the melt phase to produce more char during co-pyrolysis is also proposed.¹⁰

In order to understand if the product formation is linear with composition of cellulose:PP, the experimental product compositions are compared with the calculated ones as shown in Table 1. The calculated product composition in the case of mixtures is based on the experimental product yields from fast pyrolysis of pure cellulose and PP according to the formula, $Y_{calc.mix} = X_{cellulose}Y_{expt.cellulose} + X_{PP}Y_{expt.PP}$. Y corresponds to the yield of a particular organic compound, while $X_{cellulose}$ and X_{PP} denote the mass composition of cellulose and PP in the feed. It is clear that the formation of hydrocarbons follows the calculated composition up to C:PP ratio of 50:50. All other products deviate significantly from the calculated values, suggesting that these compounds are indeed involved in the interactions leading to the formation of new products, i.e. alcohols. Except alcohols and char, the experimental compositions of other product groups, such as anhydrosugars, carbonyl compounds and furans, are lower than that of the calculated values. Importantly, the yield of alcohols increases with increase in PP content in the feed. From Table S1 (in supplementary data), it is evident that a majority of these alcohols contain more than 7 carbon atoms and are linear, branched or cyclic. The hydrocarbon backbone of a number of these alcohols also mimics the products from pure PP pyrolysis. In order to evaluate the positive effect of co-pyrolysis on the reduction of oxygen content in the pyrolysates, the total oxygen present in the condensable fraction was evaluated based on GC/MS data of product composition. This was compared with the oxygen present in the feed mixtures. As PP does not contain oxygen, the

oxygen content in the mixture was calculated only based on cellulose $[(-C_6H_{10}O_5)_n]$. The C, H and O content in the feed mixtures and bio-oils obtained at 500 °C are tabulated in Table S7 (in supplementary data). The extent of deoxygenation was calculated as the ratio of difference between oxygen content in feed and that in bio-oil to oxygen content in feed. The extent of deoxygenation achieved in the pyrolysates was c.a. 40% for pure cellulose, while it was 67%, 73.5% and 62% for cellulose:PP mixtures of 75:25, 50:50 and 25:75 mass ratios, respectively. It is evident that the presence of optimal amount of cellulose is important to achieve high deoxygenation via dehydration, decarboxylation and decarbonylation reactions. PP rich mixture inherently contains lesser amount of oxygen, and the observed trend indicates that favorable interactions in the form of oxygen removal reactions occur in the equal composition mixture of cellulose and PP. The magnitude of deoxygenation obtained in this work is comparable with the literature. Sharypov et al.¹¹ observed nearly 90% deoxygenation in the heavy liquid fractions obtained from pyrolysis of mixtures of pine wood, beech wood and lignin with PP in a high pressure autoclave.

3.2 Effect of Temperature on Product Spectrum

Figure 2 depicts the variation of composition of different product groups formed during fast pyrolysis of cellulose:PP mixtures at different temperatures. Alcohols and hydrocarbons constitute a major fraction of the products in the temperature range of 500-700 °C. For all the mixture compositions, maximum production of hydrocarbons is observed at 600 °C, and it decreases at higher temperatures owing to the conversion of condensable long chain hydrocarbons ($>C_6$) to non-condensable hydrocarbons (C1-C3) by end-chain fission and β -scission reactions.¹² This is primarily driven by the high value of activation energy of end-chain fission reactions (70 kcal mol^{-1}),³² which are dominant at high temperatures. Alcohol production

is optimum, i.e 30-39% in the temperature range of 600-700 °C, for all the mixture compositions. Interestingly, alcohol content in the pyrolysate increases with increase in PP content in the mixture. Table S8 (in supplementary data) provides a snapshot of the individual products and their area% composition when the equal composition mixture was fast pyrolyzed at 500 °C. It is evident that a majority of the alcohols are linear saturated or unsaturated in structure, which indicates that the formation mechanism might involve the transfer of hydroxyl radicals from cellulose to PP free radicals. The formation of hydroxyl radicals from cellulose can occur during free radical mediated dehydration reaction. The β -scission of a tertiary carbon radical in any of the first to fifth position in the cellulose structure can lead to the formation of hydroxyl radicals. The formation of these radicals during gas phase pyrolysis of glycerol is reported.³³ Shen and Gu³⁴ proposed a plausible mechanism of cellulose pyrolysis involving the formation of hydroxyl, alkoxy and other carbon centered radicals. A concerted E₁ elimination pathway is also proposed in the literature for 1,2-dehydration of glucose and cellulose.³⁵⁻³⁷ As hydroxylation of PP fragments by H₂O is not possible in the absence of a catalyst, this pathway has to be disregarded over the free radical pathway. The yield of char decreases with increase in temperature for all the mixtures, which is in agreement with literature.^{20,38}

With increase in temperature, the formation of oxygenated compounds such as anhydrosugars, furan derivatives and carbonyl compounds decreased for a majority of the mixture compositions. There was no significant variation of carboxylic acids and esters with temperature, and their yield was 1-2% for all the mixtures. A clear decrease in yield of anhydrosugars with temperature was observed for cellulose:PP of 75:25, while their formation increased at higher temperatures for 50:50 and 25:75 mixture compositions. Nevertheless, the overall yield of anhydrosugars was less than 3% for these mixtures owing to the low content of

cellulose. Hydroxy- and methyl-substituted pyranones were also grouped under anhydrosugars, 1,4:3,6-Dianhydro glucopyranose was the major anhydrosugar observed at all temperatures. A similar variation was also observed for furans and their derivatives. For the equal composition mixture, furans production continuously increased with temperature that the yield was doubled at 800 °C. The formation of furans is proposed to occur via ring closing of sugars followed by dehydration reactions.^{13,39} Importantly, aldol condensation of lighter oxygenates from cellulose pyrolysis such as acetaldehyde and glycolaldehyde can lead to the formation of tetraose sugars that act as precursors for furans.⁴⁰ The yield of aldehydes and ketones varied in the range of 4-8% for 75:25 and 50:50 mixtures, while their production was less than 3% for 25:75 mixture. Importantly, the formation of benzene derivatives (monoaromatics), and polyaromatic hydrocarbons (PAHs) increased with temperature. Majority of the monoaromatics included benzene, toluene and xylene (BTX), styrene, ethyl benzene and ethyl methyl benzene, while PAHs included naphthalene, alkyl naphthalenes, acenaphthylene, indene, methyl indene, anthracene, and fluorene among other minor derivatives of the above compounds. Significant production of the above aromatics occurred only at 700 and 800 °C. Very high yields of monoaromatics (26.5%) and PAHs (24.76%) were observed at 800 °C for the equal composition mixture, while their yield was lesser for both cellulose and PP-rich mixtures.

From Figure 2, it is evident that there is a drastic decrease in alcohol and hydrocarbon yields at 800 °C for the equal composition mixture, which is also significantly lower than that for the other mixtures at the same temperature. This can be correlated with the formation of aromatic hydrocarbons. Linear hydrocarbon end-chain radicals from PP can form aromatics via 1,6-cyclization, followed by β -scission and hydrogen abstraction reactions.¹² Benzene formation is proposed to occur at high pyrolysis temperatures from linear alkenes via cyclization reaction.⁴¹

C2-C6 alkenes are formed at high temperatures (700-800 °C) via end-chain β -scission and hydrogen abstraction reactions.^{32,42} The formation of aromatics such as BTX during catalytic fast co-pyrolysis of cellulose and PP is shown to occur via Diels-Alder cycloaddition reaction between a furan derivative from cellulose and C2/C3 alkene from PP.²² Similarly, the reaction of alkenes with alcohol fragments and C2-C3 carbonyl and carboxylic acids can result in the formation of phenolic compounds. This is substantiated by the significant production of phenolic compounds (c.a. 2%) from 50:50 mixture at 800 °C. Owing to the optimum formation of cellulose and PP derived small fragments from the equal composition mixture, the yields of aromatics, PAHs, and char are high.

3.3 Quality of Co-pyrolysis Products

In order to probe the quality of the condensable fraction obtained from fast co-pyrolysis, carbon number distribution of the major products, viz. hydrocarbons, carbonyl compounds, and alcohols, are plotted (Figure 3). It is clear that cellulose-derived aldehydes and ketones fall in the carbon number range of C2-C9, whereas PP-derived hydrocarbons constitute a wide carbon number range of C3-C26. The major hydrocarbons from PP are alkyl substituted trimers (C9-C12) and hexamers (C19-C20). The various linear and cyclic hydrocarbons are listed in Table S8 (in supplementary data) for equal composition mixture at 500 °C. Interestingly, the cellulose-PP interaction products, i.e. alcohols, span a carbon range of C8-C20. An evident increase in C8-C20 alcohol content is observed with increase in PP content in the mixture at all temperatures. For example, at 600 °C, the C8-C20 alcohol content followed the order: 36.32% (C:PP 25:75) > 33.74% (50:50) > 29.57% (75:25). A similar trend was also observed for C6-C15 hydrocarbons at 600 °C: 32.82% (25:75) \approx 31.56% (50:50) > 25.38% (75:25). Importantly, high yields of alcohols and hydrocarbons are observed at 600 °C for all compositions, which shows that the

vapor phase interactions involving hydroxyl radical abstraction from cellulose, chain fission, β -scission and intramolecular hydrogen abstraction from PP chain are favorable at this temperature. This suggests that the presence of PP induces free radical reactions in cellulose, especially hydroxyl radical formation, while cellulose fast pyrolysis predominantly involves concerted reactions in the absence of PP.^{13,39} Scheme 1 depicts the plausible intermediates involved in the formation of alcohols during fast co-pyrolysis. The structures of major alcohols formed at more than 1% are also shown. From the structure of these alcohols it is evident that methyl abstraction from PP and subsequent hydrogen transfer is also a dominant pathway for the formation of less branched linear alcohols such as alkyl substituted dodecanol, octanol and decanol. The formation of long branches can also occur via free radical recombination of an end-chain with mid-chain hydrocarbon radicals.^{12,42}

In order to assess the energy content of the condensates from co-pyrolysis, higher heating value (HHV) of the condensable fraction was evaluated using the Lloyd and Davenport's formula given by, $\text{HHV (MJ kg}^{-1}\text{)} = -0.3578[\%C] - 1.1357[\%H] + 0.0845[\%O] - 0.0594[\%N] - 0.1119[\%S]$.⁴³ The percentage of C, H and O were evaluated by using the GC/MS product composition data. While there are a number of empirical formulae available in the literature to calculate HHV of a variety of feedstocks,⁴⁴ we chose this formula after testing its validity for the feed mixtures. The HHVs of the feed mixtures determined using a bomb calorimeter are listed in Table S9 (in supplementary data). Cellulose has a low heating value (15.54 MJ kg⁻¹), while PP has a very high heating value (46.47 MJ kg⁻¹). The HHVs of the mixtures increase linearly with PP content in the feed. The HHVs calculated by Lloyd and Davenport's formula for the feed mixtures matched well with experimental data. As expected, the HHV of cellulose derived bio-oil was 21.7 MJ kg⁻¹, while that from pure PP was 43.23 MJ kg⁻¹. HHVs of the pyrolysates from

the mixtures at different temperatures varied in the range of 36-41 MJ kg⁻¹ (Figure 4). This is due to long chain hydrocarbons and alcohols that contribute significantly to the H content in the oil fraction, and hence, the heating value. The energy densification ratio, defined as $\text{HHV}_{\text{oil}} / \text{HHV}_{\text{feed}}$, varied in the range of 1 to 1.5 for the oils derived from the mixtures. As alcohols, hydrocarbons and benzene derivatives constitute a major fraction (>50%) of the bio-oil components, they are expected to contribute more to the heating value, especially for the fast pyrolysis of mixtures. Therefore, we plotted the sum of yields of these components obtained from various experiments and plotted them against calculated HHVs. A striking linear correlation is evident from Figure 4, which shows that the major products contribute to an effective increase in heating value of the oil. While the recent studies on co-pyrolysis of biomass and polymers have shown that the production of aromatics can be improved by using catalysts such as zeolites,¹⁹⁻²³ our study shows that non-catalytic co-pyrolysis is a promising upstream processing technique to improve the quality of the bio-oil. Importantly, high yield of C8-C20 alcohols and C6-C15 hydrocarbons, that are valuable as gasoline range compounds are produced during fast co-pyrolysis. The co-pyrolysis bio-oil can then be subjected to catalytic HDO with possibly low hydrogen load.

3.4 Effect of Co-pyrolysis on Pyrolysis Timescale

Understanding the time evolution of products during fast pyrolysis is a key component in analytical pyrolysis studies, as it yields useful information on the time of completion of pyrolysis, vapor phase interactions, and the formation of secondary pyrolysates. However, very few studies are available in the literature on time resolved fast pyrolysis of biomass.⁴⁵⁻⁴⁷ Ultrapyrolysis,⁴⁵ pyroprobe®⁴⁶ and wire-mesh reactors⁴⁷ have been utilized for this purpose. Green and co-workers developed a semi-empirical model to describe Py-FT-IR data of corn cob

pyrolysis at different heating rates from $10\text{ }^{\circ}\text{C min}^{-1}$ to $10000\text{ }^{\circ}\text{C s}^{-1}$.⁴⁶ In this work, we utilized Py-FT-IR to unravel the reaction timescales in fast co-pyrolysis of cellulose and PP of different compositions. Figure 5 depicts the FT-IR spectra of the pyrolysis vapors from cellulose-rich (75:25) mixture at $500\text{ }^{\circ}\text{C}$ at various intervals of time from 0 to 50 s. The major functional group vibrations including O–H stretch (3431 cm^{-1}), C–H aromatic (3072 cm^{-1}) and methyl stretch (2962 cm^{-1}), $-\text{CH}_2-$ stretch of hydrocarbon backbone ($2920\text{--}2933\text{ cm}^{-1}$), C=O carbonyl stretch in aldehydes and ketones (1735 cm^{-1}), aromatic ring stretch ($1506, 1615\text{ cm}^{-1}$), C–C skeletal (1127 cm^{-1}), C–O primary alcohol stretch (1056 cm^{-1}), C–H vinyl bend (888 cm^{-1}), cyclohexane ring stretch ($990, 1010\text{ cm}^{-1}$) and CO_2 (2348 cm^{-1}) are marked. From the spectra it is clear that slight increase in absorbance of major functional group vibrations occurs at 6 s (red color curves), and after 8 s, drastic increase in absorbance is observed, corresponding to the evolution of various products. It is also evident that the time taken for maximum absorbance (or production) differs for different functional groups. For example, it takes 12 s for maximum production of primary alcohols (C–O stretch), while it takes 18–20 s for the production of linear chain hydrocarbons ($-\text{CH}_2-$ stretch). It is important to note that a broad peak corresponding to O–H stretch in $3300\text{--}3600\text{ cm}^{-1}$ range can be attributed to both water of dehydration and alcohols formed during fast co-pyrolysis. In order to quantify the time evolution of various functional groups for fast pyrolysis of cellulose, PP and their mixtures, the absorbance or peak height was plotted with time (Figure 6). A flat FT-IR spectrum obtained at the start of pyrolysis (0 s) ensured that no external interferences from the purge gas affected the product spectra.

Figures 6(a)–6(e) depict the time evolution of major component vibrations for cellulose, PP and the mixtures. For cellulose pyrolysis, the intensity of carbonyl and primary alcohol vibrations are higher than other functional groups, suggesting that C=O and –OH groups present

in C2-C4 alcohols, aldehydes, ketones, furan derivatives like furfural, 5-hydroxymethyl furfural and furanones, carboxylic acids, and anhydrosugars such as pyranones and levoglucosenone, are produced in high amounts. This is also in good agreement with the products identified from GC/MS (Tables S1-S6 in supplementary data). Importantly, the maximum production of the major products occurs at 12-14 s. Except carbonyl vibration, the intensity of other functional groups are steady after 16 s, suggesting that a majority of the products bearing alcohol functional groups evolve even at much longer timescales (30-40 s). These might include C2-C3 oxygenates such as hydroxy acetaldehyde (glycolaldehyde), hydroxy acetone (acetol), oxo acetic acid (glyoxylic acid) and 2-oxo propanoic acid (pyruvic acid), which are obtained in significant amounts during cellulose fast pyrolysis at 500 °C (Tables S2 and S4 in supplementary data). This shows that during cellulose fast pyrolysis, dehydration of pyranose units along with cellulose chain initiation and depropagation are the dominant reactions^{13,39} in the initial time periods, while the formation of C2-C3 oxygenates via secondary transformation of dehydrated C4-C6 sugars via retro-Diels-Alder and retro-aldol reactions^{13,39} occur at longer timescales.

The addition of PP to cellulose results in the formation of the same functional groups, albeit at very different intensities and pyrolysis times. As depicted in Figure 6(b), the addition of 25% of PP to cellulose results in decrease in intensity of carbonyl vibration and a concomitant increase in $-\text{CH}_2-$ vibrations arising from the hydrocarbon backbone. Unlike pure cellulose fast pyrolysis, all the peaks tend to decrease after reaching maxima signifying the decrease in concentration of the functional groups. This shows that the incorporation of PP tends to accelerate the completion of pyrolysis. The profile of $-\text{CH}_2-$ vibration exhibits two humps, one at 15 s and another at 20 s. The earlier hump matches with the time corresponding to maximum evolution of primary alcohols, indicating that long chain alcohols are formed as a result of

hydroxyl radical interaction between cellulose and PP. The second hump is expected to correspond to the evolution of hydrocarbons from PP. An increase in PP composition in the mixture leads to interesting changes in the evolution of products. From Figures 6(c) and 6(d), it is clear that the time taken for maximum production of various functional groups decreases significantly to 10 s, and all the functional group peak heights decrease to zero, signifying faster completion of pyrolysis compared to cellulose and cellulose-rich mixture. Based on the intensity of the vibrations, the functional groups can be arranged as follows: $-\text{CH}_2-$ (hydrocarbons) > O–H (water + alcohols) > CO_2 > C=O (carbonyl/acids) > C–O (primary alcohols). The profiles of methylene stretching vibration for equal composition (50:50) and PP-rich (25:75) mixtures are very similar to that for pure PP pyrolysis (Figure 6(e)). It can be observed that the intensity of O–H stretching vibration is higher than C–O stretching vibration exhibited by primary alcohols, especially when PP content is equal or higher in the mixture. This suggests that increasing the PP content in the mixture leads to higher extent of dehydration via hydroxyl and hydrogen shift reactions. It can hence be concluded that besides improving the quality of the condensable fraction in terms of the production of long chain alcohols and hydrocarbons, co-pyrolyzing PP with cellulose decreases the time for completion of the reaction significantly. This will lead to better conversion of the feedstock in larger scale reactors.

Figure 6(f) depicts the concentration profiles of CO and CH_4 measured using an online gas analyzer. The timescales corresponding to the evolution of these gases do not exactly match with the timescale of the condensates owing to the residence time of the gases in the tubing leading to the gas analyzer. Nevertheless, the CH_4 evolution is similar to the trend exhibited by $-\text{CH}_2-$ vibration at different cellulose:PP compositions. A clear shift in maximum concentration of CH_4 to shorter time periods is observed for equal composition and PP-rich mixtures, which

reconfirms the trends observed in FT-IR profiles. Thus alcohol and hydrocarbon production occur simultaneously at short timescales during co-pyrolysis. CO evolution starts even before the evolution of CH₄, which shows that cellulose begins to pyrolyze via concerted reactions even before free radical formation from PP could occur. CO evolution is high for cellulose-rich mixtures, and it increases with 25% addition of PP. It is also worthwhile to note that the intensity of CO₂ vibration increases significantly for 50:50 and 75:25 mixtures compared to that for cellulose-rich mixtures (Figures 6(c) and 6(d)). These results show that deoxygenation occurs predominantly via decarbonylation and decarboxylation during co-pyrolysis. An ensemble of the above observations suggest that co-pyrolyzing biomass with polymers is a promising option to improve deoxygenation, and hence, the quality of bio-oil. Importantly, this is the first work to show the time evolution of key functional groups during fast co-pyrolysis and evaluate the effects of cellulose:PP composition on reaction timescales and provide qualitative insights on product formation mechanisms and interactions between cellulose and PP. More rigorous studies on characterization and stability of bio-oil from fast co-pyrolysis of actual biomass and commercial plastics will aid in commercialization of this process.

4. Conclusions

In this work, the potential of co-pyrolysis of biomass and polymers to produce high quality biofuels is demonstrated. Experiments performed with various compositions of cellulose and PP in Py-GC/MS shows that long chain alcohols (C8-C20) are formed as the major products of interaction between the two feed components. The alcohol content increased with PP content in the mixture, and highest alcohol yield of 36% was achieved with 25:75 C:PP mixture at 600 °C. High yield of C6-C15 hydrocarbons (c.a. 34%) was also produced with PP-rich mixtures at 500 and 600 °C. High temperatures led to the production of monoaromatic and poly aromatic

hydrocarbons with a concomitant decrease in char content. Heating values of the bio-oils obtained from fast pyrolysis of the mixtures were in the range of 36-41 MJ kg⁻¹, and a linear correlation between heating value and total composition of alcohol, aliphatic and aromatic hydrocarbons was observed. Deoxygenation is promoted via decarboxylation and decarbonylation reactions. For the first time, the effect of cellulose:PP composition on time evolution of key functional groups was assessed using Py-FT-IR, and the presence of PP was found to significantly decrease the time of completion of fast pyrolysis by more than 10 s. Transfer of hydroxyl groups from cellulose to PP is proposed to be the main reaction leading to the formation of alcohol besides the concerted reactions of cellulose and free radical chain reactions of PP degradation.

Acknowledgments

The authors thank Department of Science and Technology (DST), India, for funding the project via grant no. SR/S3/CE/074/2012. The National Center for Combustion Research and Development is sponsored by DST, India.

References

1. C. Liu, H. Wang, A.M. Karim, J. Sun, and Y. Wang, *Chem. Soc. Rev.*, 2014, **43**, 7594–7623.
2. P.K. Kanaujia, Y.K. Sharma, M.O. Garg, D. Tripathi, and R. Singh, *J. Anal. Appl. Pyrol.*, 2014, **105**, 55–74.
3. P.R. Patwardhan, J.A. Satrio, R.C. Brown, B.H. Shanks, *Bioresour. Technol.*, 2010, **101**, 4646–4655.
4. J.P. Diebold, A review of the chemical and physical mechanisms of the storage stability of fast pyrolysis bio-oils. <http://www.nrel.gov/docs/fy00osti/27613.pdf> (accessed Dec. 2014).
5. A. Shihadeh, and S. Hochgreb, *Energy Fuels*, 2002, **16**, 552–561.
6. S. Wan, and Y. Wang, *Front. Chem. Sci. Eng.*, 2014, **8**, 280–294.
7. Q. Zhang, J. Chang, T. Wang, and Y. Xu, *Energy Convers. Manag.*, 2007, **48**, 87–92.
8. T.V. Choudhary, and C.B. Phillips, *Appl. Catal. A: Gen.*, 2011, **397**, 1-12.
9. F.D. M. Mercader, P.J.J. Koehorst, H.J. Heeres, S.R.A. Kersten, and J.A. Hogendoorn, *AIChE J.*, 2011, **57**, 3160–3170.
10. D.V. Suriapparao, D.K. Ojha, T. Ray, and R. Vinu, *J. Therm. Anal. Calorim.*, 2014, **117**, 1441–1451.
11. V.I. Sharypov, N.G. Beregovtsova, and B.N. Kuznetsov, *J. Anal. Appl. Pyrol.*, 2003, **67**, 325-340.
12. R. Vinu, and L.J. Broadbelt, *Annu. Rev. Chem. Biomol. Eng.*, 2012, **3**, 29-54.
13. R. Vinu, and L.J. Broadbelt, *Energy Environ. Sci.*, 2012, **5**, 9808-9826.
14. V.I. Sharypov, N. Marin, N.G. Beregovtsova, S.V. Baryshnikov, B.N. Kuznetsov, V.L. Cebolla, and J.V. Weber, *J. Anal. Appl. Pyrol.*, 2002, **64**, 15–28.
15. N. Marin, S. Collura, V.I. Sharypov, N.G. Beregovtsova, S.V. Baryshnikov, B.N. Kutnetzov, V. Cebolla, and J.V. Weber, *J. Anal. Appl. Pyrol.*, 2002, **65**, 41–55.
16. B.N. Kuznetsov, V.I. Sharypov, S.A. Kuznetsova, V.E. Taraban'ko, and N.M. Ivanchenko, *Int. J. Hydrogen Energy*, 2009, **34**, 7051–7056.
17. E. Jakab, and M. Blazso, *J. Anal. Appl. Pyrol.*, 2001, **59**, 49–62.
18. J.D. Martínez, A. Veses, A.M. Mastral, R. Murillo, M.V. Navarro, N. Puy, A. Artigues, J. Bartrolí, and T. García, *Fuel Proc. Technol.*, 2014, **119**, 263-271.

19. H. Zhang, J. Nie, R. Xiao, B. Jin, C. Dong, and G. Xiao, *Energy Fuels*, 2014, **28**, 1940–1947.
20. X. Li, J. Li, G. Zhou, Y. Feng, Y. Wang, and G. Yu, *Appl. Catal. A: Gen.*, 2014, **481**, 173–182.
21. C. Dorado, C.A. Mullen, and A.A. Boateng, *ACS Sustainable Chem. Eng.*, 2014, **2**, 301–311.
22. C. Dorado, C.A. Mullen, and A.A. Boateng, *Appl. Catal. B: Environ.*, 2015, **162**, 338–345.
23. B. Zhang, Z. Zhong, K. Ding, and Z. Song, *Fuel*, 2015, **139**, 622–628.
24. H. Zhou, C. Wu, J.A. Onwudili, A. Meng, Y. Zhang, and P.T. Williams, *RSC Adv.*, 2015, **5**, 11371–11377.
25. A. Fullana, J.A. Contreras, R.C. Striebich, and S.S. Sidhu, *J. Anal. Appl. Pyrol.*, 2005, **74**, 315–326.
26. J.K. Schneider, M.E. da Cunha, A.L. dos Santos, G.P.S. Maciel, M.C. Brasil, A.R. Pinho, F.L. Mendes, R.A. Jacques, and E.B. Caramão, *J. Chromatogr. A*, 2014, **1356**, 236–240.
27. Direct pyrolysis/FT-IR: An alternative sampling system. <http://www.cdsanalytical.com/appnotes/25.pdf> (Accessed May 2015).
28. Parameter optimization in pyrolysis/FT-IR. <http://www.analytix.co.uk/wp-content/uploads/2015/02/Parameter-optimisation-in-pyrolysis-FTIR.pdf> (Accessed May 2015).
29. Y.-C. Lin, J. Cho, G.A. Tompsett, P.R. Westmoreland, and G.W. Huber, *J. Phys. Chem. C*, 2009, **113**, 20097–20107.
30. X. Zhou, M.W. Nolte, H.B. Mayes, B.H. Shanks, and L.J. Broadbelt, *Ind. Eng. Chem. Res.*, 2014, **53**, 13274–13289.
31. S. Tsuge, H. Ohrani, and C. Watanabe, *Pyrolysis-GC/MS handbook of synthetic polymers*, Elsevier, Oxford, U.K., 2011.
32. T.M. Kruse, H.-W. Wong, and L.J. Broadbelt, *Macromolecules*, 2003, **36**, 9594–9607.
33. Y.S. Stein, and M.J. Antal Jr., *J. Anal. Appl. Pyrol.*, 1983, **4**, 283–296.
34. D.K. Shen, and S. Gu, *Bioresour. Technol.*, 2009, **100**, 6496–6504.
35. P.W. Arisz, and J.J. Boon, *J. Anal. Appl. Pyrol.*, 1993, **25**, 371–385.
36. G.R. Ponder, G.N. Richards, and T.T. Stevenson, *J. Anal. Appl. Pyrol.*, 1992, **22**, 217–229.

37. H.B. Mayes, M.W. Nolte, G.T. Beckham, B.H. Shanks, and L.J. Broadbelt, *ACS Sustainable Chem. Eng.*, 2014, **2**, 1461-1473.
38. K. Wang, K.H. Kim, and R.C. Brown, *Green Chem.*, 2014, **16**, 727-735.
39. X. Zhou, M.W. Nolte, H.B. Mayes, B.H. Shanks, and L.J. Broadbelt, *Ind. Eng. Chem. Res.*, 2014, **53**, 13274-13289.
40. S. Nie, J. Huang, J. Hu, Y. Zhang, S. Wang, C. Li, M. Marcone, and M. Xie, *Food Sci. Human Wellness*, 2013, **2**, 87-92.
41. A.M. Dean, *J. Phys. Chem.*, 1990, **94**, 1432-1439.
42. E. Ranzi, M. Dente, A. Goldaniga, G. Bozzano, and T. Faravelli, *Prog. Energy Combust. Sci.*, 2001, **27**, 99-139.
43. W.G. Lloyd, and D.A. Davenport, *J. Chem. Educ.*, 1980, **57**, 56-60.
44. J.M. Vargas-Moreno, A.J. Callejón-Ferre, J. Pérez-Alonso, and B. Velázquez-Martí, *Renew. Sust. Energy Rev.*, 2012, **16**, 3065-3083.
45. R.G. Graham, M.A. Bergougnou, and B.A. Freel, *Biomass Bioenergy*, 1994, **7**, 33-47.
46. J. Feng, Q. YuHong, and A.E.S. Green, *Biomass Bioenergy*, 2006, **30**, 486-492.
47. E. Hoekstra, W.P.M. van Swaaij, S.R.A. Kersten, and K.J.A. Hogendoorn, *Chem. Eng. J.*, 2012, **191**, 45-58.

List of Figures

Figure 1. Composition of pyrolysates when cellulose, polypropylene and their mixtures of different compositions were pyrolyzed at 500°C.

Figure 2. Effect of temperature on composition of major products formed during fast co-pyrolysis of C:PP of different compositions.

Figure 3. Effect of temperature and cellulose:PP composition on carbon number distribution of the major products in bio-oil.

Figure 4. Variation of HHV of bio-oil with sum of alcohols, hydrocarbons and benzene derivatives yield in bio-oil. The data is inclusive of all experiments performed.

Figure 5. FT-IR spectra of vapor generated from pyrolysis of C:PP 75:25 at 500 °C.

Figure 6. Time evolution of key functional groups during fast pyrolysis of (a) pure cellulose, (b) C:PP 75:25, (c) C:PP 50:50, (d) C:PP 25:75, and (e) pure PP at 500 °C in Pyroprobe®-FT-IR set-up. 6(f) shows the concentration profiles of methane and carbon monoxide for different feedstock compositions. CH₄ formation was not observed for pure cellulose pyrolysis and CO formation was not observed for pure PP pyrolysis.

List of Schemes

Scheme 1. Proposed mechanism for the formation of alcohols during fast co-pyrolysis of cellulose and PP.

List of Tables

Table 1. Comparison between the experimental and calculated composition of the major products formed during fast co-pyrolysis of cellulose and PP of different compositions at 500 °C.

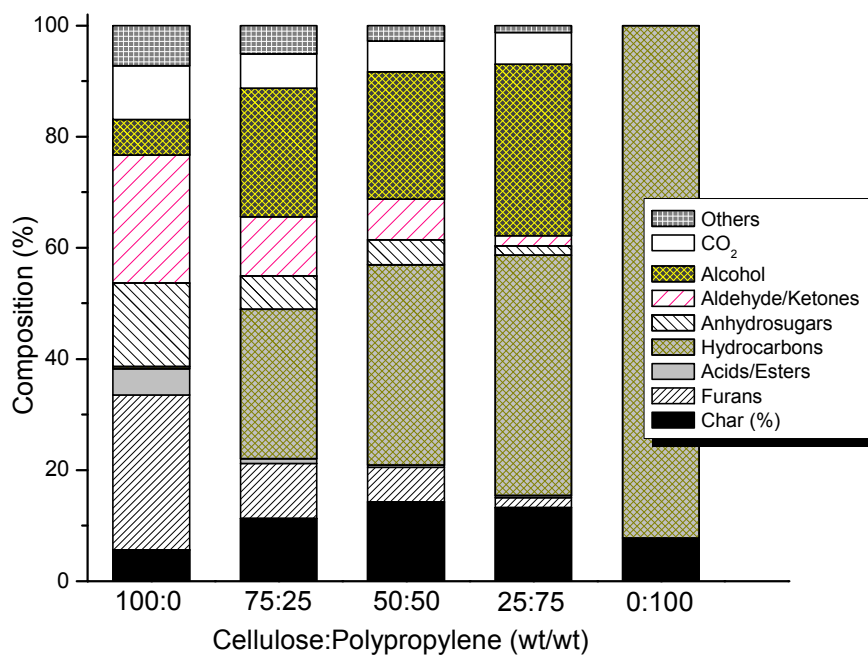


Figure 1. Composition of pyrolysates when cellulose, polypropylene and their mixtures of different compositions were pyrolyzed at 500°C.

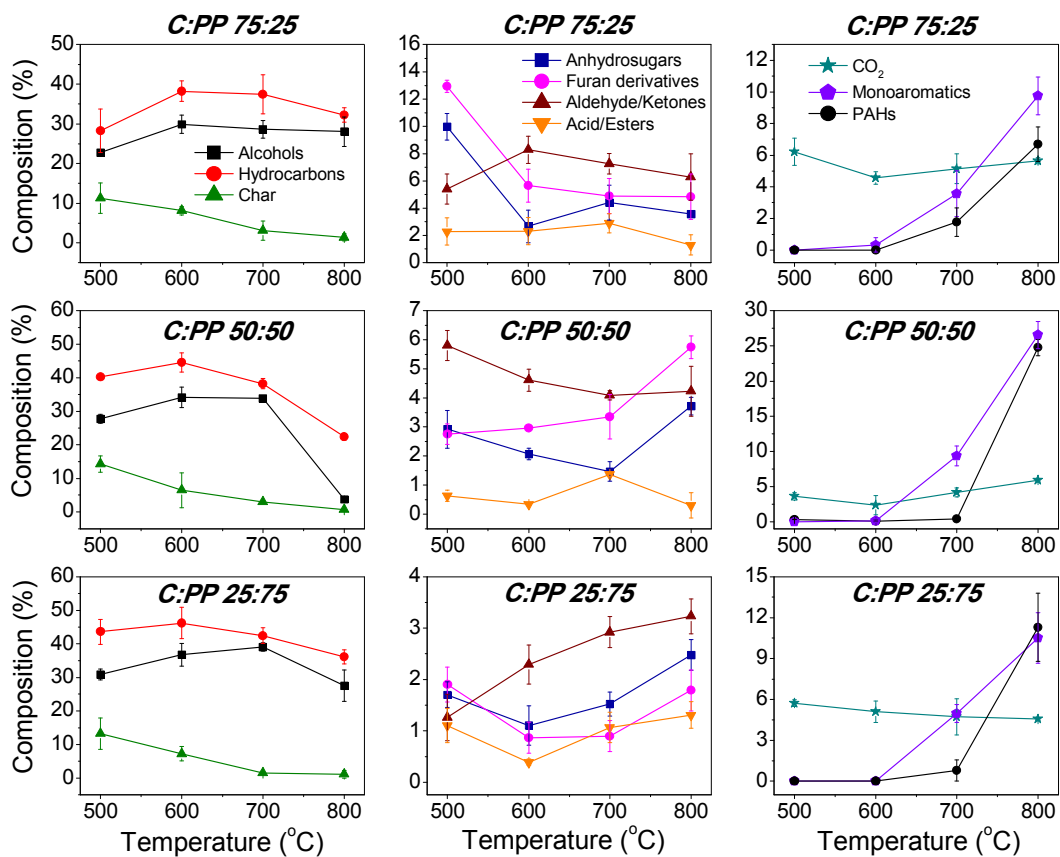


Figure 2. Effect of temperature on composition of major products formed during fast copyrolysis of C:PP of different compositions.

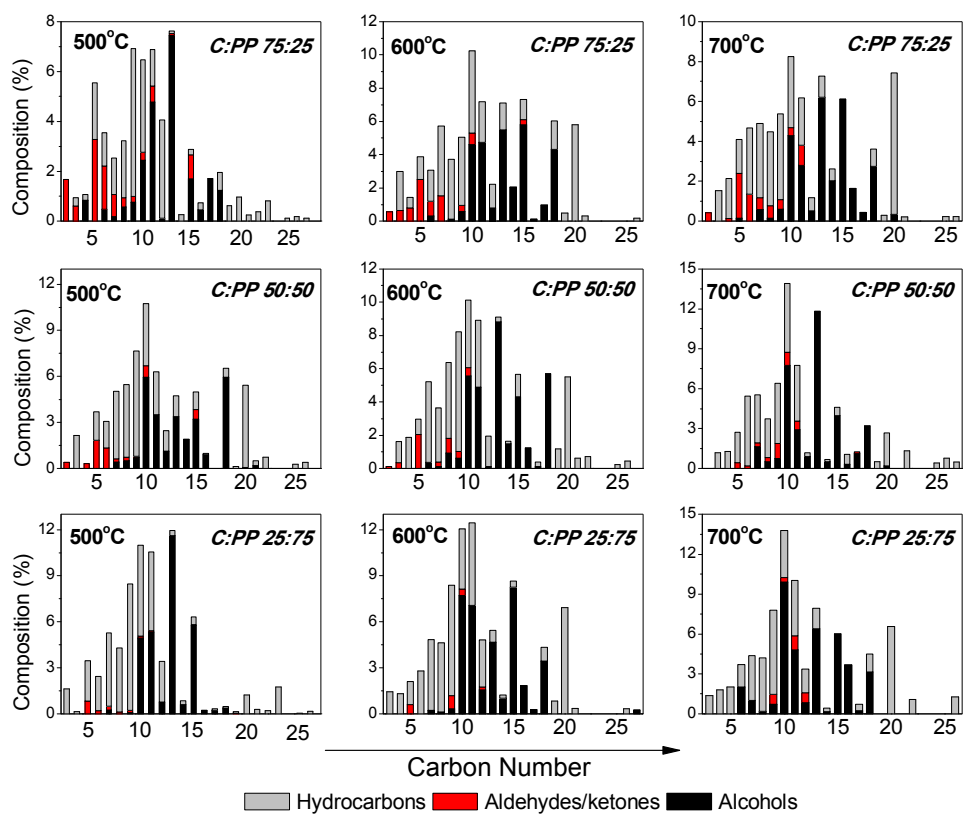


Figure 3. Effect of temperature and cellulose:PP composition on carbon number distribution of the major products in bio-oil.

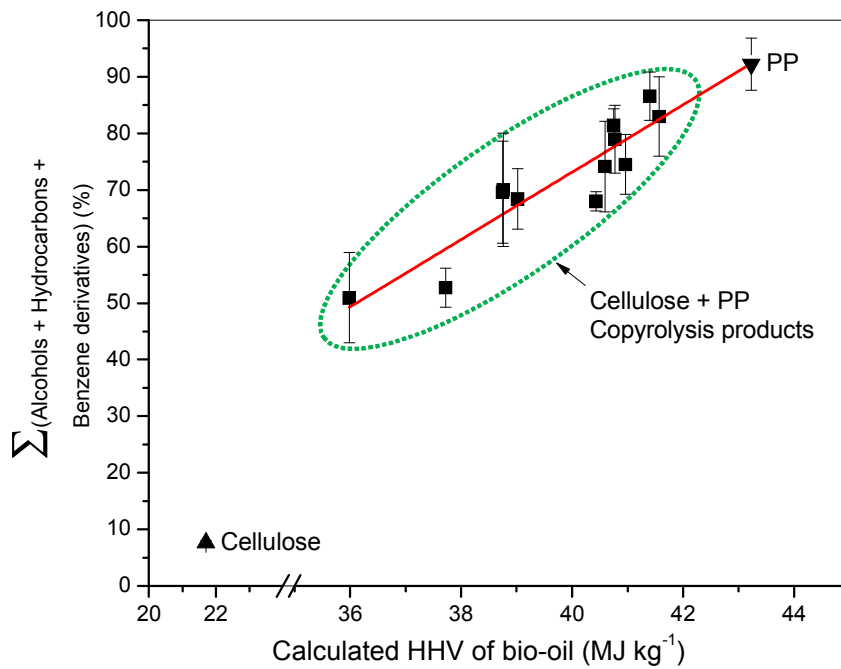


Figure 4. Variation of HHV of bio-oil with sum of alcohols, hydrocarbons and benzene derivatives yield in bio-oil. The data is inclusive of all experiments performed. The calculated HHV of bio-oil is on a dry basis.

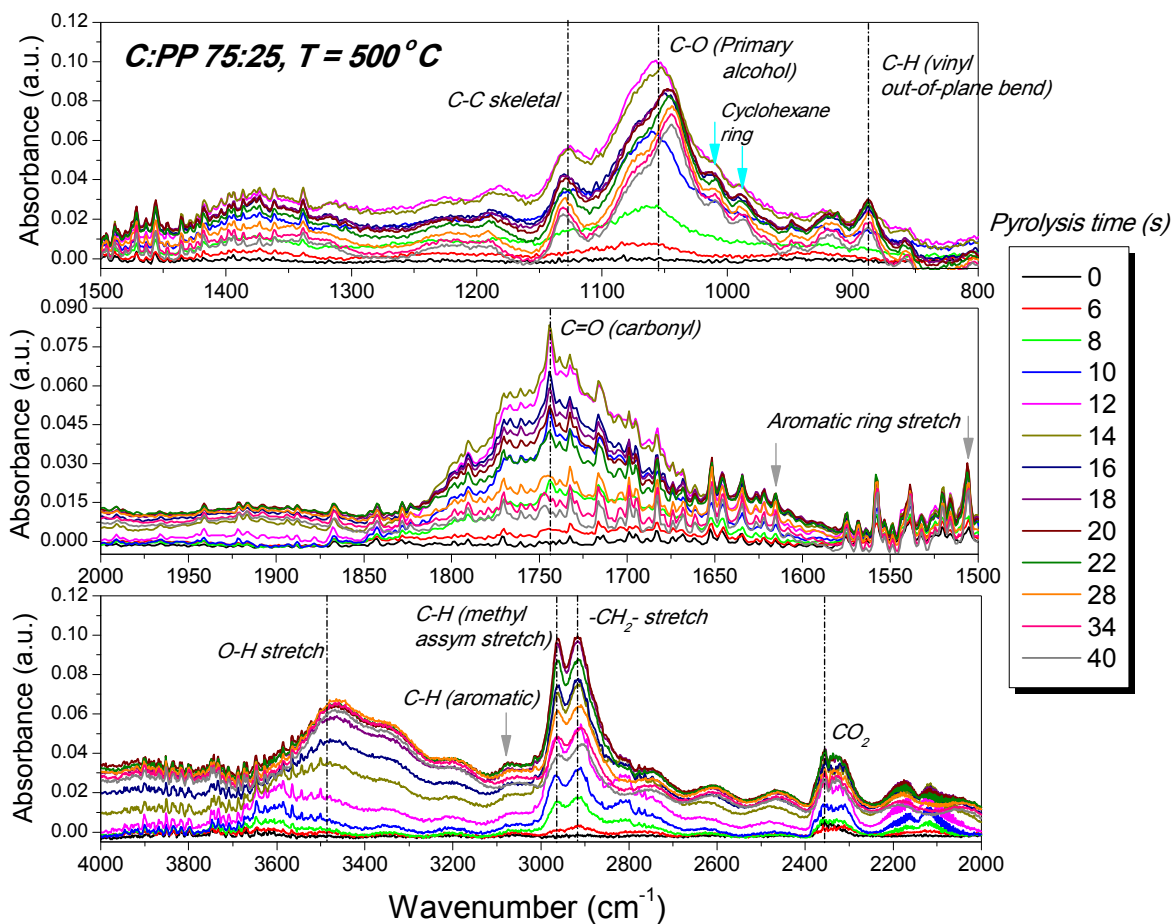


Figure 5. FT-IR spectra of vapor generated from pyrolysis of C:PP 75:25 at 500°C .

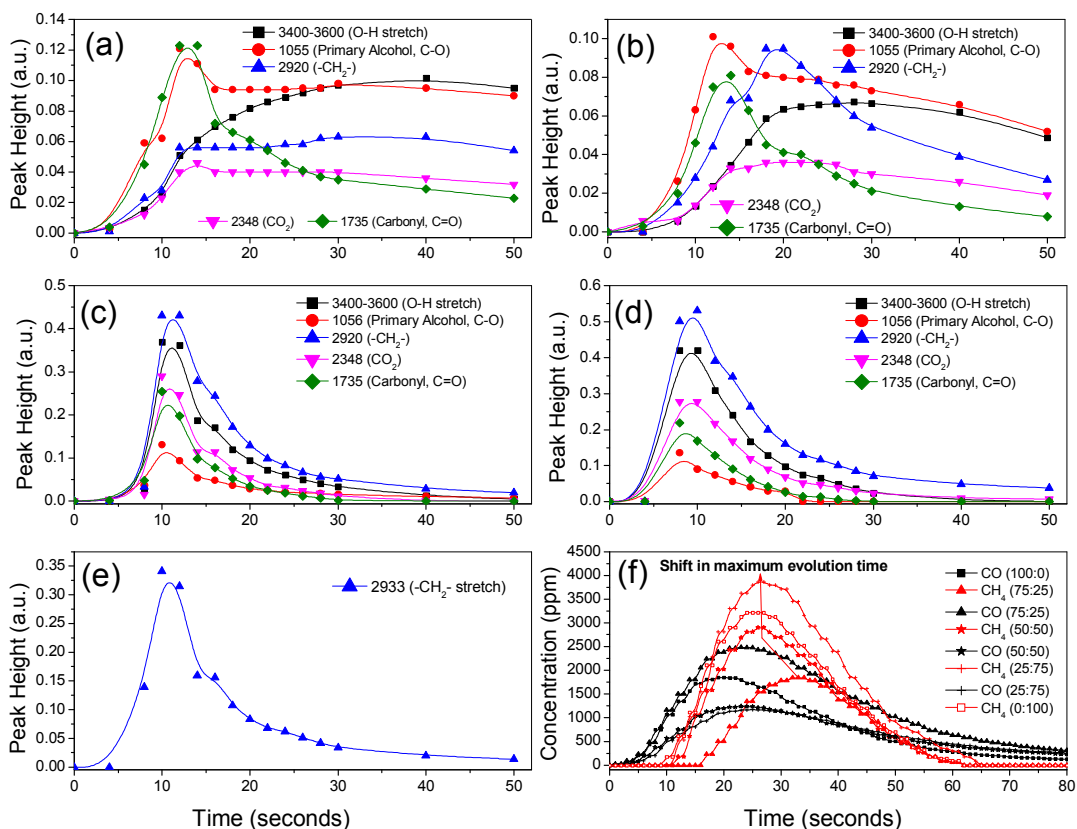
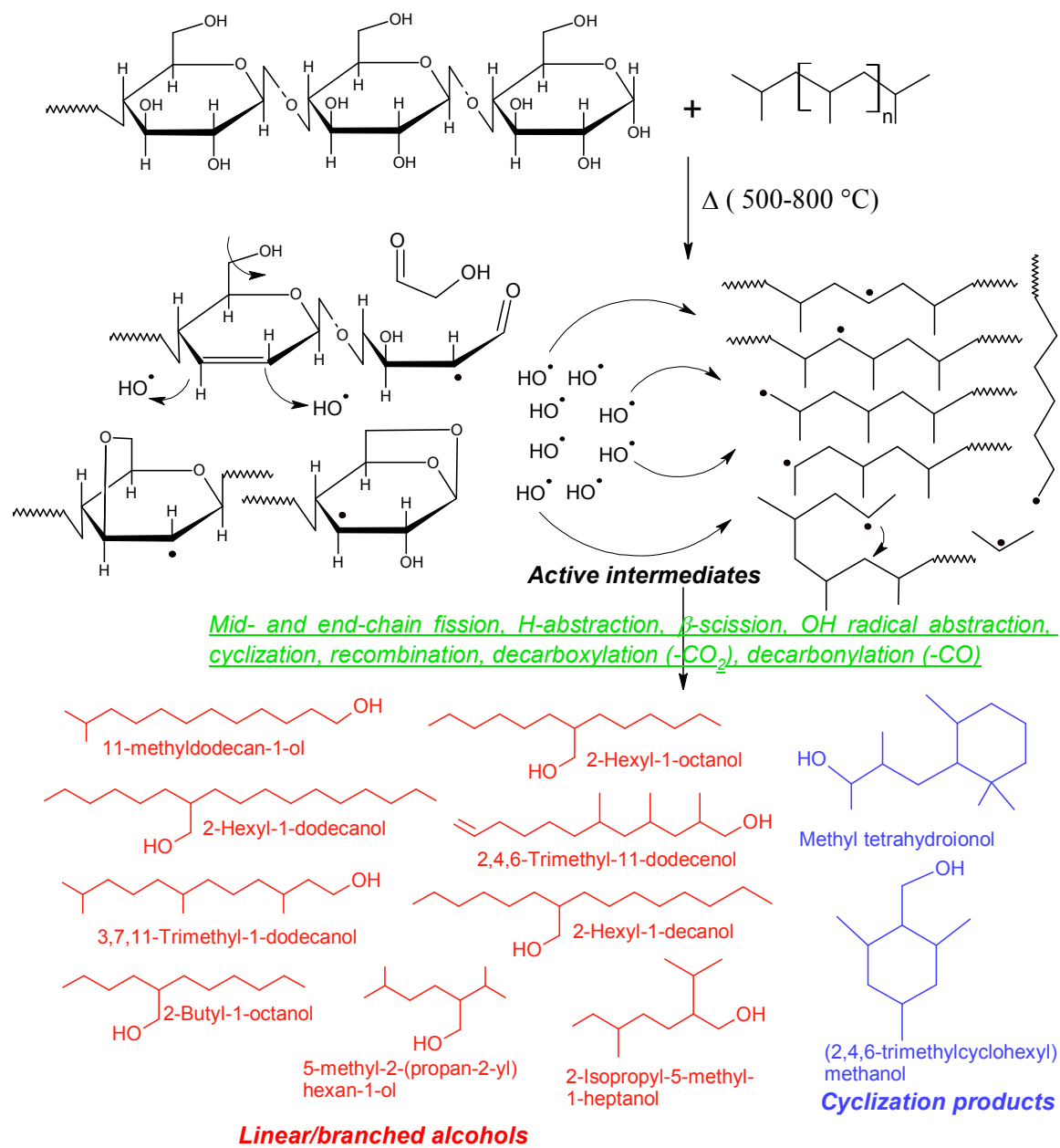


Figure 6. Time evolution of key functional groups during fast pyrolysis of (a) pure cellulose, (b) C:PP 75:25, (c) C:PP 50:50, (d) C:PP 25:75, and (e) pure PP at 500 °C in Pyroprobe®-FT-IR set-up. 6(f) shows the concentration profiles of methane and carbon monoxide for different feedstock compositions. CH₄ formation was not observed for pure cellulose pyrolysis and CO formation was not observed for pure PP pyrolysis.



Scheme 1. Proposed mechanism for the formation of alcohols during fast co-pyrolysis of cellulose and PP.

Table 1. Comparison between the experimental and calculated composition of the major products formed during fast co-pyrolysis of cellulose and PP of different compositions at 500 °C.

Feed Composition	C:PP 100:0	C:PP 75:25	C:PP 50:50	C:PP 25:75	C:PP 0:100			
Products	<i>Expt.</i>	<i>Expt.</i>	<i>Calc.</i>	<i>Expt.</i>	<i>Calc.</i>	<i>Expt.</i>	<i>Calc.</i>	<i>Expt.</i>
Alcohols	6.95	22.73	5.21	27.81	3.48	30.87	1.74	0
Hydrocarbons	0.67	28.23	23.56	40.21	46.44	43.65	69.33	92.20
Anhydrosugars	17.36	7.11	13.02	2.92	8.68	1.70	4.34	0
Aldehydes/Ketones	23.20	10.63	17.40	5.80	11.60	1.83	5.80	0
Furans	27.89	9.92	20.92	6.20	13.95	1.76	6.97	0
Char	5.67	11.29	6.20	14.32	6.73	13.28	7.27	7.80

The calculated composition was evaluated using the formula given by $Y_{calc.mix} = X_{cellulose}Y_{expt.cellulose} + X_{PP}Y_{expt.PP}$.

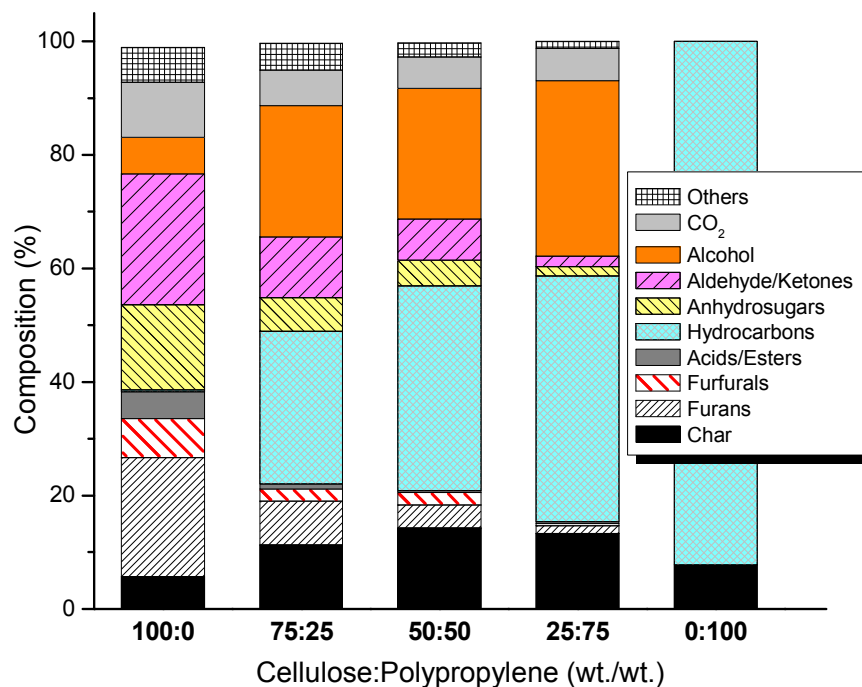
Fast Co-Pyrolysis of Cellulose and Polypropylene Using Py-GC/MS and Py-FT-IR

Deepak Kumar Ojha ^a and R. Vinu ^{a,b,*}

^aDepartment of Chemical Engineering, Indian Institute of Technology Madras, Chennai-600036, India

^bNational Center for Combustion Research and Development, Indian Institute of Technology Madras, Chennai- 600036, India

Graphical and Textual Abstract



This work features the production of C8-C20 long chain alcohols and hydrocarbons from fast pyrolysis of cellulose-polypropylene mixtures. Co-pyrolysis brings down the pyrolysis completion time in addition to enhancing the HHV and H/O ratio in bio-oil.

* Corresponding Author, Phone: +91-44-2257 4178, E-mail: vinu@iitm.ac.in (R. Vinu)